Evidence of Momentum Conservation at the Au/Si(111) Interface using Ballistic-electron-emission Microscopy

L. D. Bell

Center for Space Microelectronics Technology
Jet Propulsion Laboratory
California Institute of Technology
Pasadena, CA 91109

BEEM spectroscopy has been performed at room temperature and at 77K on Au/Si(111) structures. Au thickness was varied in the range 75-300 Å. At 77K a direct signature of parallel momentum conservation is observed in the BEEM spectra of samples with thick Au layers. The change in spectral shape which was observed as a function of both Au thickness and temperature places restrictions on allowable values of inelastic and elastic mean-free paths. The observations also suggest the presence of multiple reflections of the injected electrons within the Au layer. An independent indication of these multiple reflections is observed in the dependence of BEEM current on Au thickness in Au/Si(100) structures. Calculations provide good agreement with observed BEEM spectra and attenuation length data.

PACS Numbers: 73.50.Gr, 73.30.+y, 73.61.At, 61.16.Ch

introduction

The notion of parallel momentum ($k_{||}$) conservation at a metal/semiconductor (M/S) interface is basic to many device structures. In developing conceptual models to characterize these devices, the choice to assume or neglect $k_{||}$ conservation is often made without direct experimental verification. In epitaxial semiconductor/semiconductor or M/S structures, the concept is more straightforward, since in these cases atomically abrupt interfaces can be achieved between materials with matching lattice nets. Even here, quantitative verification is difficult, and defects may serve to obscure the signature of $k_{||}$ conservation, The failure to observe by conventional methods the effects of the predicted metal band-gap in the epitaxial $CoSi_2/Si(111)$ system [1] is one possible example of insensitivity to $k_{||}$ conservation and of the likely predominance of small defective areas in macroscopic measurements. The observation of resonant levels in a metal layer is another indicator of coherent transport and specular reflection, although a complete understanding of intensities is required to rule out a diffuse component.

The problem of determining the presence or lack of $k_{||}$ conservation in the case of a non-epitaxial evaporated metal film has a long history and is considerable y more problematical. In this case, $k_{||}$ conservation has been difficult to confirm, Contributing to the difficulty is the insensitivity y of conventional measurements to the degree of $k_{||}$ conservation. Macroscopic probes of M/S structures, such as current-voltage and internal photoemission measurements are spatially averaged methods of probing interface transport, and measurements maybe dominated by interface defects. In addition, elastic scattering within the bulk of the layer, either with phonons or with defects, can in many cases eliminate characteristics associated with interface momentum conservation. In general, the problem is one of separating a lack of $k_{||}$ conservation, in the form of elastic interface scattering, from other scattering processes.

The development of ballistic-electron-emission microscopy [2] (BEEM), based on scanning tunneling microscopy [3] (STM), has provided a nanometer-scale technique for probing interface electronic properties and electron transport through heterostructures. BEEM uses an STM tip to inject hot carriers, usually within several eV of the Fermi level, into a M/S structure. By detecting the collected current (I_c) which enters the semiconductor as a function of injection energy (tip voltage), a spectroscopy of electron transport and interface electronic properties may be performed. In addition, these characteristics can be imaged with high spatial resolution. However, even BEEM measurements have been inconclusive in determining the degree of $k_{||}$ conservation at non-epitaxial M/S interfaces; an unambiguous signature of this characteristic has so far remained elusive.

One of the first predictions for BEEM based on the idea of $k_{||}$ conservation was the spectrum for metal/Si(1 11) [4], which was expected to differ dramatically from that of metal/Si(l 00). Si(111) spectra were expected to show a more gradually increasing threshold region and a substantially different spectral shape. The modified spectral behavior calculated for the Si(1 11) orientation is due to the mismatch between the off-axis conduction-band minima in the Si and the forward-focused electron distribution produced by tunneling. At electron energies only slight] yin excess of the Schottky barrier height, few electrons are injected from the STM tip with sufficient $k_{||}$ to enter the Si conduction band. As the tunnel voltage and electron energies increase, the phase space for transport into the conduction band increases and extends toward the interface Brillouin zone center and consequently toward smaller values of $k_{||}$. This produces a stronger overlap with the injected electron distribution and causes the collected current to increase more quickly. Calculated spectra for Au/Si(100) and Au/Si(1 11) are plotted in Fig. 1. The calculation involves phase-space considerations only, and does not include scattering. in addition, each electron is given only one chance for collection; if phase space restrictions are not satisfied on the first attempt, the electron is lost.

This predicted behavior has not previously been observed for Au/Si(111). Instead, previously reported BEEM spectra [4] are nearly identical to those for Au/Si(100). This observation, however, does not disprove interface $k_{||}$ conservation. While it is likely that scattering of some type is responsible for this result, elastic scattering in the metal film can provide the necessary parallel momentum for electrons to enter the Si(111) conduction-band minima, even if $k_{||}$ is conserved at the interface. It is the presence of bulk scattering which has made the identification of $k_{||}$ conservation so difficult previously. A measurement is needed which separates the various scattering components and any effects of metal band structure and allows interface processes to be assessed independently. This paper describes the observation of $k_{||}$ conservation at a M/S interface by BEEM, even when standing waves and coherent transport within the metal are not observed.

Experimental Procedures

In order to test these ideas, a series of spectra from Au/Si(111) samples was obtained as a function of Au thickness, both at room temperature and at 77K. Si substrates were prepared by performing a solvent clean, followed by spin-etching [5] and hydrogen termination of the Si surface using 1:10 HF:ethanol in a nitrogen-purged glove-box. Following direct transfer of the sample into a load-lock and thence to the ultra-high vacuum deposition chamber, Au evaporation was performed at a base pressure of 10^{9} Torr and monitored by quartz crystal oscillator. Uncertainty in Au thickness was ±10%. Several samples were fabricated for each Au thickness, and many spectra from these samples were averaged together for analysis. BEEM results were reproducible bet ween similar sets of averaged spectra, although some variation was observed if the averages were small. Acquisition of BEEM spectra was performed in a nitrogen-purged glove-box, and low temperature measurements were accomplished by direct immersion of the BEEM system in liquid nitrogen, also within this glove-box. Tunnel current was maintained at

either 1 or 2 nA for all BEEM spectra; BEEM spectra presented in this paper were normalized to a common tunnel current of 1 nA.

Results and Discussion

A summary of the spectroscopy results for three Au thicknesses is presented in Fig. 2. At room temperature, the spectral shape above threshold remains constant, as does the threshold position, which is a measure of Schottky barrier height V_b. The solid lines, produced by fitting the spectra near threshold with the original BEEM phase-space model, emphasize this behavior. This phase-space model provides an excellent fit to BEEM spectra for the case of Au/Si(100), where there are Si conduction-band states at $k_{||}=0$. The agreement of the plotted fits with the present data is due to the fact that the Au/Si(111) spectrum shape closely matches that of Au/Si(100), a result which was previously observed. The inflection of the data at higher voltages as Au thickness increases results from an increasing contribution from scattering, in particular from the energy dependence of inelastic scattering.

At 77K the spectrum shape, even near threshold, changes dramatically with increasing Au thickness; because of this changing shape, the apparent threshold increases substantially. Near-threshold fits are also shown for these spectra as a reference to the changing shape, although they are clearly inappropriate for the spectra obtained for the thicker Au layers. These fits are provided as a qualitative means of tracing the change in spectral shape and the increase of the apparent spectral threshold. There is a smooth transition of spectral shape with Au thickness at both temperatures.

Although threshold values from these fits are given in Fig. 2, it is important to emphasize that the Schottky barrier height is not changing as a function of Au thickness at 77K. The M/S interface is already fully developed with a Au layer of 75 Å; a further increase of Au thickness

does not modify this barrier height. The fact that the phase-space model incorrectly assigns the barrier height at 77K in Fig. 2 is an indication that it is inadequate for the low-temperature data In addition, although the fits to the threshold regions of the 77K spectra appear- adequate at thicker Au layers, this is only because the fit is over a small range of voltage. The shape of the entire spectrum for these cases is quite different from the more conventional Au/Si(100) spectrum.

In summary, Fig. 2 indicates that (a) fit quality and threshold position (-0.82 V) at room temperature are reasonable and identical to Si(100); (b) fit quality and threshold position (0.88 V) at 77K for thin Au are also reasonable, and near to that (0,86 V) of Si(100); and (c) fit quality and threshold position (0.94 V) at 77K for 300Å Au are strongly anomalous.

The observed change in spectral shape at 77K is an unexpected result. The Au/Si(111) spectra which are obtained for the thickest Au layers strongly resemble those expected for the (111) orientation only with no elastic scattering and for $k_{||}$ conservation at the M/S interface. There are several points to emphasize concerning these observations. First, this behavior only appears at low temperature, and only for thicker Au layers, whereas it might be expected that increased scattering in thick Au layers would preclude this observation. However, the evolution of spectrum shape at low temperature cannot be attributed to a modification of the hot electron distribution by increased scattering in the Au, since spectra for Si(100) do not show this behavior. Moreover, spectra obtained at room temperature, where scattering is expected to be stronger, do not exhibit this behavior for either substrate orientation.

It is also important to note that Au band structure effects are unlikely to be responsible for these modified spectra. Evaporated Au has been observed to be primarily of[111] orientation on both Si(100) and Si(111) [6, 7]; only the 77K Si(111) results display this strong change in spectral shape. Moreover, such effects would not produce the observed evolution of spectral shape at

such thick Au layers. Au band structure is well-developed at 75 Å, and further change in the range of 75-300 Å is not expected. 'I'he large change in spectral shape observed at low temperature occurs in this thickness range.

Secondly, the effect of temperature on the BEEM spectra could not easily be resolved in terms of band structure. The primary effect of temperature on BEEM is to change the sample lattice temperature, which affects the phonon population, Thus scattering by phonon absorption and stimulated emission will depend on temperature, The effect of metal band structure could be twofold: to direct the electrons along certain directions in the metal, and to provide a mismatch with the semiconductor band structure at the M/S interface. These conditions, which could lead to a change in spectral shape, would be effective regardless of temperature and phonon population. Clearly, the anomalous spectral shape in the present BEEM spectra appears only at low temperature.

Mention should be made of the recent work by Garcia-Vidal et al. [8], which introduces a theoretical model based on Au band structure effects to explain Au/Si(111) BEEM results. While this model represented a reasonable explanation of prior Au/Si(111) spectra, it appears to be a less probable description in light of the new data presented here. Previously obtained Au/Si(1 11) BEEM spectra were essentially identical to those for Au/Si(1 00). However, the present work provides experimental evidence that Au/Si(111) spectra can be quite different under appropriate conditions.

Finally, an explanation involving a change in the physical structure of the Au layer with thickness also appears unlikely, No systematic change in surface grain structure was observed by STM as a function of Au thickness.

It is possible to construct a consistent conceptual model for the results of Fig. 2. It should first of all be pointed out that inelastic electron-electron scattering will usually remove an electron from the collection process altogether, since the energy lost is large, with a distribution which peaks at one-half of the electron's kinetic energy. [9] A significant contribution to the collector current from inelastically scattered electrons would thus not be expected until $V - 2V_b$ -1.6 V. Therefore, elastic scattering is the important process in the modification of the momentum distribution of collectable electrons. The only interpretation consistent with these observations is that, at 77K, elastic scattering is decreasing as the Au layer gets thicker. The contributions of nearly all components of scattering (electron-phonon, electron-electron, impurity, and defect scattering) will increase with metal thickness. One contribution, scattering from the metal film boundaries, will decrease with film thickness, since as the boundaries are separated the electrons encounter thcm less frequently. Thus the dominant source of elastic scattering and momentum randomization at low temperature must be diffuse reflection from the Au surface, implying multiple passes of the hot electrons within the Au film. Full boundary-to-boundary transport must be involved, since the effects of this randomization on the BEEM spectrum decrease only as the boundaries are separated. It is not required that the surface reflection be locally diffuse, since many BEEM spectra are averaged together. Averaging over different surface gradients will provide an average diffuseness to the reflected distribution.

This averaging over Au surface topography implies that there should be some degree of variation from spectrum to spectrum. This would be expected particularly for the spectra in which surface reflections play an important role in determining spectral shape (thinner layers at low temperature). Specifically, although surface reflection is treated as diffuse in an average sense, it might be specular in a local sense. If the tip is situated over a flat area parallel to the M/S interface, surface reflection might provide little change in parallel momentum, and most electrons might still not be able to enter the Si(1 11) conduction-band minima, In this case, the (local) spectrum should resemble the 77K thick-Au case (that is, shifted threshold and anomalous shape).

In contrast, spectra taken over rough topography could resemble "conventional" Au/Si(100) BEEM spectra (or room-temperature Au/Si(111) spectra).

Figure 3 presents two averages of small subsets of 77K data from a 75 Å sample, which represent two extreme cases. Also shown are simple phase-space fits near threshold (as in Fig. 2), and threshold values are also given, It is clear that variation is observed. Interestingly, thresholds range from 0.86 V (the most commonly observed value for these smaller averages, and the usual value at 77K for Au/Si(100)) to 0.93 eV, nearly as large as the 77K 300 Å average shown in Fig. 2(f). The shapes also vary from that of Au/Si(100) to that of Fig. 2(f). These are exactly the limits expected under the assumptions of the model.

Specular reflection at the M/S interface is assumed here, in order to be consistent with $k_{||}$ conservation and absence of scattering upon transmission. High-resolution cross-sectional transmission electron microscopy (TEM) was performed in order to characterize the Au/Si(111) interface. Images reveal a large-height step structure with flat terraces. The steps often were observed to form (100) facets, This stepped topography is quite different from the interface character previously observed for Au/Si(100). [10] In that case, large areas of flat topography were not often observed. The TEM results suggest that a smooth Si(111) surface is more resistant to reaction with Au than the (100) surface. Similarly, in BEEM experiments on Au-covered Si(111) (7x7) surfaces, Cuberes et al. [11] did not observe the effects of diffusion,

This model for the data can thus be summarized as follows. At low temperature, the elastic mean-free path λ_e for electron-phonon scattering is greatly increased. In contrast, inelastic electron-electron scattering is largely independent of temperature. [12] Inelastic scattering primarily removes electrons from the collection process altogether, as mentioned above. For thin Au layers, electrons which are not initially collected may reflect from the M/S interface and reach the surface, where they scatter, Because the Au is thin, these electrons are able to make several

passes through the film before being removed by inelastic scattering. 'I"he electrons are randomized by this surface scattering, which allows many more to be subsequently collected. Thus the BEEM spectrum for Au/Si(1 11) resembles the Au/Si(1 00) spectrum.

As Au thickness increases, fewer electrons are able to make multiple passes through the Au, and the average momentum randomization decreases. For 300 Å Au layers, very few electrons survive to be reflected back to the surface and then be collected, so collection is due primarily to electrons collected on their first attempt. Thus the spectrum is that expected for Si(1 11) in the absence of elastic scattering.

At low temperature, the Au surface is the primary source of elastic scattering. At room temperature, the stronger quasi-elastic scattering due to electron-phonon interactions randomizes the injected electrons, especially for thicker Au layers. Surface scattering is no longer required for randomization, although these multiple reflections still occur for thinner layers.

Calculations and Modeling

In order to determine appropriate scattering parameters for the array of BEEM spectra in Fig. 2, the standard technique of Monte Carlo simulation was used. In these simulations, 106 electrons were injected per voltage point. A Schottky barrier height of 0.82 eV was used at room temperature; 0.86 eV was used at 77K. These values are derived from BEEM measurements on Au/Si(1 00); the increase at low temperature results from the change in the Si band gap. A free-electron model was assumed for the Au layer, and an effective-mass model was used for the Si collector, with six elliptical conduction-band minima situated near the X-points. Mass components of $0.98m_e$ and $O.19m_e$ were used.

At 77K, electron-phonon scattering was neglected. First, λ_i was selected to obtain the best fit simultaneously to all 77K spectra. It was simplest to perform this fit to the 77K spectra first, and then add phonon scattering to the model for the room-temperature data. The low temperature observations place limits on the allowable value of the inelastic mean-free path λ_i. This must be long enough to allow multiple electron passes for 75 Å Au, but short enough so as to usually allow only one collection attempt at 300 Å Au. An additional restriction is imposed by the observed total attenuation length for Au of about 130 Å as measured by BEEM at room temperature. [13] The expression $1/\lambda_{tot} = 1/\lambda_i + 1/\lambda_c$ relates λ_i and λ_c to the total attenuation length λ_{tot} measured by BEEM for moderate Au coverages. The Monte Carlo modeling indicates that this relation holds for thick Au layers, but not for thin layers; this will be discussed in detail later. Thus λ_i and λ_c must each be greater than 130& but one of the two must be smaller than about 260 Å.

There is a large body of early work on hot-electron mean-free paths in Au, Internal photoresponse experiments by Crowell at al. [14] yielded a value $\lambda_{tot} = 740$ Å for 1 eV electrons in Au. Subsequently Stuart et al. [15] performed Monte Carlo calculations which were consistent with that experimental data. Soshea and Lucas [16] noted a correction to Crowell's optical absorption calculations which produced a much smaller value of $\lambda_{tot} = 380$ Å in Au. The overestimation of attenuation lengths present in these optical experiments reflected the uncertainties in modeling the optical absorption. BEEM provides a direct method for measuring attenuation length which is not subject to these uncertainties. In BEEM, injected current is known exactly, and the spatial origin of this current (the Au surface) is also controlled. The initial BEEM measurement of $\lambda_{tot} = 130$ Å for -1 eV electrons at moderate Au coverages has been reproduced by several groups. [17, 18] Other BEEM modeling on different material systems, such as Pd/Si [19], has also extracted values for λ_i and λ_c. In that case, values were derived which were consistent with the shorter λ_{tot} for Pd of about 31 Å.

Several additional considerations which have been included in the model for the Monte Carlo calculations should be mentioned. λ_i is assumed to be energy-dependent, a property which causes the increasing inflection with Au thickness of the room temperature spectra. However, the theoretical $1/(E-E_F)^2$ dependence [9] is too strong to be consistent with the experimental spectra. Other BEEM experiments have also measured a weaker dependence. [19] For the calculations presented here, a weaker linearly decreasing energy dependence of $\lambda_i = 1.5 \cdot \lambda_{i0}(1-(E-E_F)/3)$ is used, where energies are in electron volts and λ_{i0} is the mean-free path for electrons at $E-E_F = 1$ eV. This empirical expression was found to provide a consistently good fit to the high-voltage portions of the BEEM spectra. The particular functional form is not critical to the modeling of the threshold region, since the choice primarily affects the higher voltage inflection of the spectra.

λ_c is assumed to be quasi-elastic and energy-independent for these energies. [20] Also, no elastic impurity or defect scattering is included. Such a contribution must be small to allow observation of the spectral behavior displayed by the 300 Å data at low temperature. Boundary reflections are assumed to be specular at the M/S interface and diffuse at the Au surface, as mentioned above. STM images of the Au surfaces reveal the typical mounded structure of evaporated Au films, indicating that, on average, diffuse reflection from these surfaces is reasonable.

Quantum mechanical reflection contributes an energy-dependence to interface transmission, This contribution, calculated for a sharp-step potential, is included for the low-temperature spectra. At high temperature, Lee et al. [21] find little energy dependence when phonon backscattering in the semiconductor is also included. In this case, only an overall scale factor of-0.5 results. [22] This scale factor is included for the room temperature data.

Planar tunneling [23] is used for the initial electron injection from the STM tip. A more realistic treatment has been introduced for the non-planar STM geometry. [24] For a 3 eV work.

function, that theory yields a tunneling gap of s--6 Å at a tunnel voltage of about 1 V. Lang et al. [25] have pointed out that an energy width of-O.2 eV is expected for the tunneling distribution in the non-planar model. In the planar tunneling model a value of s= 15 Å, which has been previously used [2] to fit BEEM spectra, reproduces this energy width. This value ofs is used here.

In order to fit both the 75 Å and 300 Å data at 77K, a narrow range of λ_i proved to be suitable. A secondary restriction was imposed by the observed magnitude of I_c. Excessively large or small values of λ_i produced calculated currents much smaller or larger than observed. It is encouraging that the range of λ_i which provided the most consistent fit to the spectral shapes of the 77K data also generated values of I_c which were in agreement with the observed currents. The best overall series of fits was produced using λ_i=220 Å. A value of λ_c=400 Å was then selected to model the room-temperature spectra. This value was dictated by the chosen value of λ_i and by the observed total attenuation!engthof-130 Å for moderate Au thicknesses (50 -200 Å). An error of 20% is estimated for the values of λ_i and λ_c; a change in these parameters by this amount results in a substantial disagreement with one or more of the experimental spectra.

Figure 4 shows the resultant fits to the BEEM spectra from Fig. 2. The change in shape at low temperature is reproduced by the calculations, leading to an apparent increase in threshold. The addition of elastic scattering also reproduces the room temperature measurements. In addition, the calculated I_c magnitudes agree well with the measured values, the ratio of the two being close to 1:1 for all spectra.

The conceptual model presented here depends critically on the mechanism of multiple electron passes through the Au layer. There is a compelling additional indication of multiple reflections and of the validity of this model. In a separate series of experiments, a sequence of Au/Si samples was fabricated using Si(100) substrates, including samples with Au layers as thin as

14 Å. BEEM current attenuation as a function of Au thickness for these samples at room temperature yields a dependence which deviates from simple exponential behavior for thinner Au layers, as shown in Fig. 5. Using the same model which was used to fit the individual BEEM spectra in Fig. 4, a calculated attenuation curve is generated which is also plotted as a solid line in Fig. 5. Since the λ_c and λ_i values have been chosen to match the measured λ_{tot} for thicker layers, the agreement in slope there is expected. The notable feature is that the calculation reproduces the deviation at thin layers extremely well. This behavior is a direct result of the inclusion of multiple electron reflections within the Au layer, The width and shape of this "peaking" calculated for small layer thicknesses is determined by the attenuation lengths used, and depends on no additional adjustable parameters. When multiple reflections are not allowed, the calculated dependence lacks this characteristic, as shown by the dashed line in Fig. 5.

It is of interest to note that the chosen values of λ_i and λ_c imply a total attenuation length of λ_{tot}= 142 Å, slightly larger than the observed value of 130 Å. Previous measurements which assumed strict exponential behavior between 50 and 200 Å were probably affected slightly by the deviation from exponential behavior for thin Au layers. In fact, fitting of the data in Fig. 5 between 50 and 300 Å (since a 200 Å point is not available in this data set) to a pure exponential yields an attenuation length of 128 Å, exactly that which was derived in previous work. [13, 26]

It is important to realize that this evidence of multiple electron reflections is a completely independent measurement from those previously discussed, and over a different thickness range. The signature shape at thin Au layers displayed by this plot occurs mainly at Au thicknesses of less than 100 Å, whereas the change in spectrum shape in Figs. 2 and 4 occurs primarily at thicknesses greater than 100 Å.

Interestingly, Niedermann et al. [27] observed an apparently shorter mean-free path at thinner PtSi layers in BEEM measurements of PtSi/Si(100) structures. They also observed this

behavior in reverse BEEM [28] data. They interpreted as an interracial layer with a shorter attenuation length; however, it appears possible that this was also an observation of multiply reflected electrons.

Conclusions and Acknowledgements

These BEEM measurements have provided direct evidence of a strong degree of $k_{\|}$ conservation for hot electrons crossing the Au/Si(1 11) interface. The signature of this process only occurs at low temperature, and only with thick Au layers. The dependence of BEEM spectral shape on Au thickness indicates that multiple electron passes within the Au layer are contributing to collected current. This contribution has obscured interface momentum conservation in previous low-temperature experiments with thinner Au layers. In addition, independent evidence of multiple electron passes has been detected in BEEM attenuation length measurements. Although a contribution from diffuse transmission may exist at certain locations due to defects, these results indicate that the average contribution from such a component to interface transmission must be relatively small. Shape and magnitude of the spectra are well-fit by the present model; a substantial diffuse transmission contribution would quickly alter the characteristic spectral shape observed at low temperature for thick Au layers.

TEM imaging by T. George is gratefully acknowledged. The research described in this paper was performed by the Center for Space Microelectronics Technology, Jet Propulsion Laboratory, California Institute of Technology, and was jointly sponsored by the Office of Naval Research and the Ballistic Missile Defense Organization / Innovative Science and Technology Office through an agreement with the National Aeronautics and Space Administration (NASA). The Cray supercomputer used in this research was provided by funding from the NASA Offices of Mission to Planet Earth, Aeronautics, and Space Science.

References

1. L. F. Mattheiss and D. R. Hamann, Phys. Rev. B 37, 10623 (1988).
2. W. J. Kaiser and L. D. Bell, Phys. Rev, Lett. 60, 1406 (1988); L. D. Bell and W. J. Kaiser, Phys. Rev. Lett. 61,2368 (1988).
3. G. Binnig, H. Rohrer, Ch. Gerber, and E. Weibel, Phys. Rev. Lett. 49, 57 (1982).
4. L. J. Schowalter and E. Y. lee, Phys. Rev. B 43, 9308 (1991).
5. P. J. Grunthaner et al., Thin Solid Films 183, 197 (1989).
6. K. Ours and T. Hanawa, Surf Sci. 82, 202(1979).
7. A, K. Green and E. Bauer, J. Appl. Phys. 47, 1284 (1976).
8. F. J. Garcia-Vidal, P. L. de Andres, and F. Flores, Phys. Rev. Lett. 76, 807 (1996).
9. R. H. Ritchie and J. C. Ashley, J. Phys. Chem. Solids 26, 1689 (1965).
10. L. D. Bell, A. M. Milliken, S. J. Manion, W. J. Kaiser, R. W. Fathauer, and W. T. Pike, Phys. Rev. B 50, 8082(1994).
11. M. T. Cuberes, A. Bauer, H. J. Wen, M. Prietsch, and G. Kaindl, Appl. Phys. Lett. 64, 2300 (1994).
12. J. J. Quinn, Phys. Rev. 126, 1453 (1962).
13. M. H. Hecht, L. D. Bell, W. J. Kaiser, and F. J. Grunthaner, Appl. Phys. Lett. 5S, 780 (1989).
14. C. R. Crowell, W. G. Spitzer, L. E. Howarth, and E. E. LaBate, Phys. Rev. 127,2006 (1962).
15. R, N. Stuart, F. Wooten, and W. E. Spicer, Phys. Rev. Lett. 10, 7 (1963).
16. R. W. Soshea and R. C. Lucas, Phys. Rev. 138, Al 182(1965).
17. H. Palm, M. Arbes, and M. Schulz, Appl. Phys. A Solids Surf. **A56, 1 (1993).**
18. C. A. Ventrice, V. P, LaBella, G. Ramaswamy, H.-P. Yu, and L. J. Schowalter, Phys. Rev. B S3, 3952(1996).
19. R. Ludeke and A. Bauer, Phys. Rev. Lett. 71, 1760 (1993).

20. S. M. Sze, J. L. Moll, and T. Sugano, Solid State Electron. 7, 509(1964).

21. E. Y. lee and L. J. Schowalter, J. Appl. Phys. 70,2156 (1991).

22. C. R, Crowell and S. M. Sze, in *Physics of Thin Films, Vol.* 4, edited by G. Haas and R. E. Thun (Academic Press, New York, 1967), pp. 325-371.

23. J. G. Simmons, J. Appl. Phys. 34, 1793 (1963).

24. J. Tersoff and D. R. Hamann, Phys. Rev. Lett. 50, 1998(1983).

25. N. D. Lang, A. Yacoby, and Y. Imry, Phys. Rev. Lett. 63, 1499 (1 988).

26. L. D, Bell, W. J. Kaiser, M. H. Hecht, and L. C. Davis, in *Scanning Tunneling Microscopy,* edited by J. A. Stroscio and W. J. Kaiser (Academic Press, San Diego, 1993), p. 333.

27. P. Niedermann, L. Quattropani, K. Solt, A. D. Kent, and O. Fischer, J. Vat. Sci. Technol. B **10,** 580 (1992).

28. L. D. Bell, M. H. Hecht, W, J. Kaiser, and L. C. Davis, Phys. Rev. Lett. 64, 2679(1990).

Figure, Captions

Figure 1 Calculated BEEM spectra for metal/Si(1 00) (squares) and metal/Si(l 11) (circles), neglecting scattering and boundary reflections in the metal film. The two curves have been plotted with different scale factors for clarity.

Figure 2 Experimental BEEM spectra (circles) obtained for Au/Si(1 11) samples. Also shown by solid lines are fits to the data using the original BEEM phase-space model for Au/Si(1 00), which neglects scattering. Pitting is only to data points at tunnel voltages ≤ 1.2 V.

Figure 3 Averages of two small subsets of the group of spectra which produced Fig. 2(d). The variation observed for these subsets is expected from variations in Au surface topography, and the behavior varies between the limits expected from the model.

Figure 4 Experimental BEEM spectra (circles) shown in Figure 2. The solid lines are fits to the data using the Monte Carlo model described in the text. The Monte Carlo calculations have been adjusted only by an overall scale factor in order to obtain a best fit to the data. This scale factor ranges from 0.98 to 1.04 for the spectra.

Figure 5 Experimental BEEM attenuation length measurement (circles) for Au/Si(1 00) samples, For each point, I_c was measured at V = 1.2 V. Also shown (solid line) is the dependence calculated from the same Monte Carlo model used to fit the experimental BEEM spectra in Fig 2. This calculated curve has been adjusted only by an overall vertical offset, corresponding to a scale factor of 1.28. The dashed line is the dependence which results if electrons are allowed only one attempt to cross the M/S interface; that is, if boundary reflections within the Au film are not allowed.

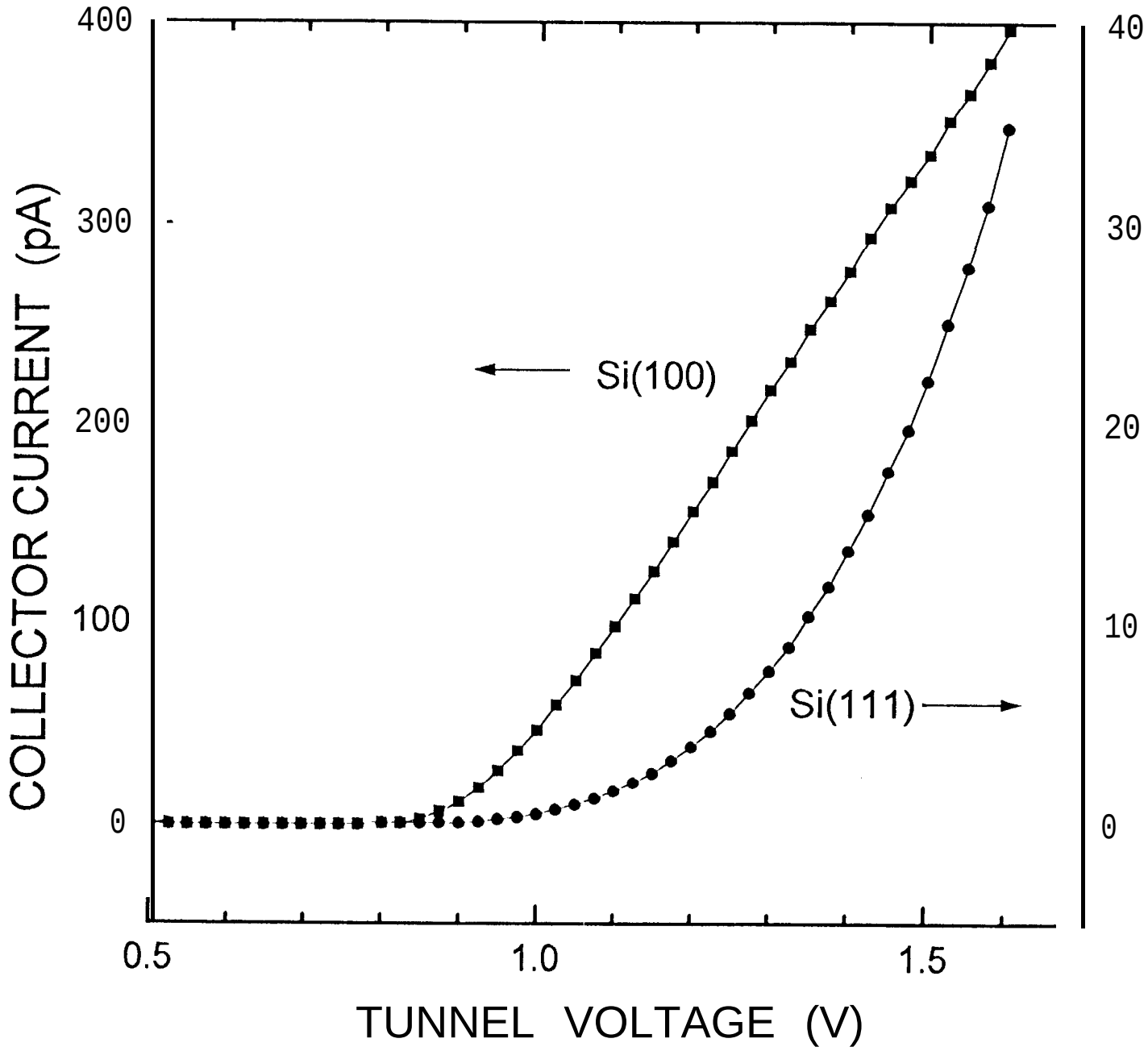
400
300
200
100
0
40
30
20
10
0
COLLECTOR CURRENT (pA)
Si(100)
Si(111)
0.5
1.0
1.5
TUNNEL VOLTAGE (V)

Figure 1

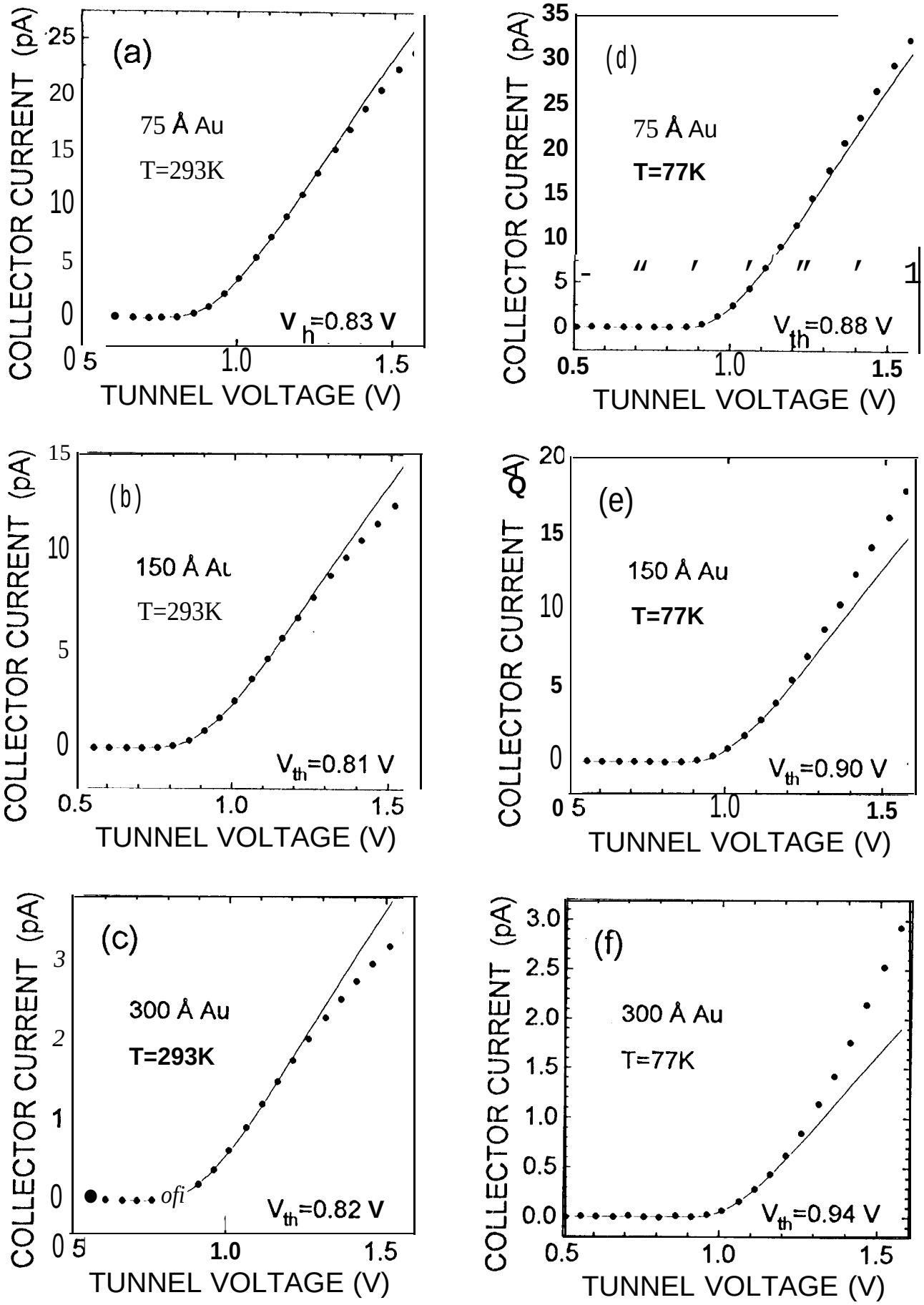
(a)
75 Å Au
T=293K
V h=0.83 V
COLLECTOR CURRENT (pA)
TUNNEL VOLTAGE (V)
(d)
75 Å Au
T=77K
V th=0.88 V
COLLECTOR CURRENT (pA)
TUNNEL VOLTAGE (V)
(b)
150 Å Au
T=293K
V th=0.81 V
COLLECTOR CURRENT (pA)
TUNNEL VOLTAGE (V)
(e)
150 Å Au
T=77K
V th=0.90 V
COLLECTOR CURRENT (pA)
TUNNEL VOLTAGE (V)
(c)
300 Å Au
T=293K
V th=0.82 V
COLLECTOR CURRENT (pA)
TUNNEL VOLTAGE (V)
(f)
300 Å Au
T=77K
V th=0.94 V
COLLECTOR CURRENT (pA)
TUNNEL VOLTAGE (V)

Figure 2

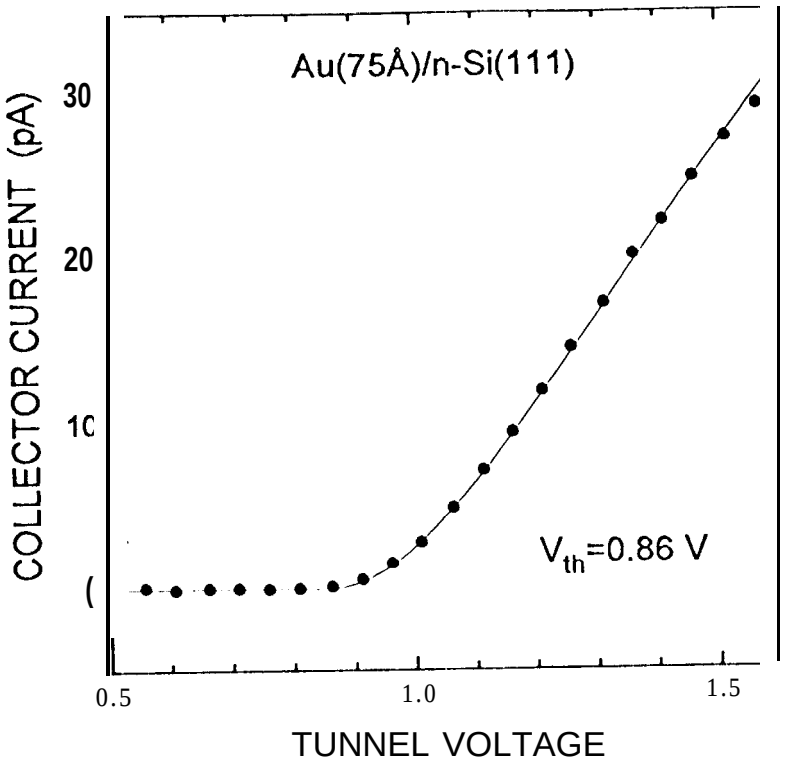
Au(75Å)/n-Si(111)
COLLECTOR CURRENT (pA)
30
20
10
(
V_{th}=0.86 V
0.5
1.0
1.5
TUNNEL VOLTAGE

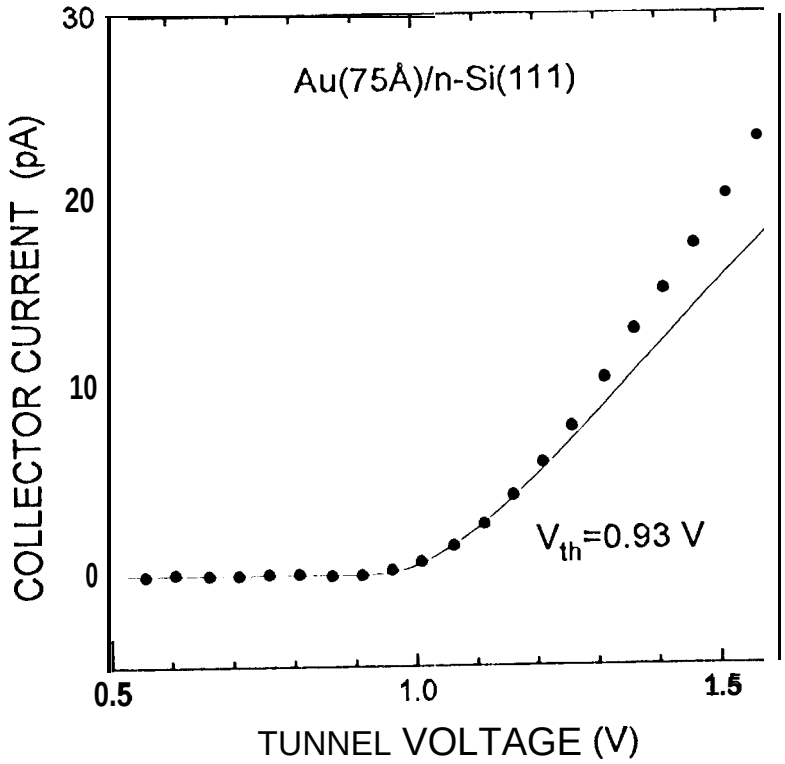
Au(75Å)/n-Si(111)
COLLECTOR CURRENT (pA)
30
20
10
0
V_{th}=0.93 V
0.5
1.0
1.5
TUNNEL VOLTAGE (V)

Figure 3

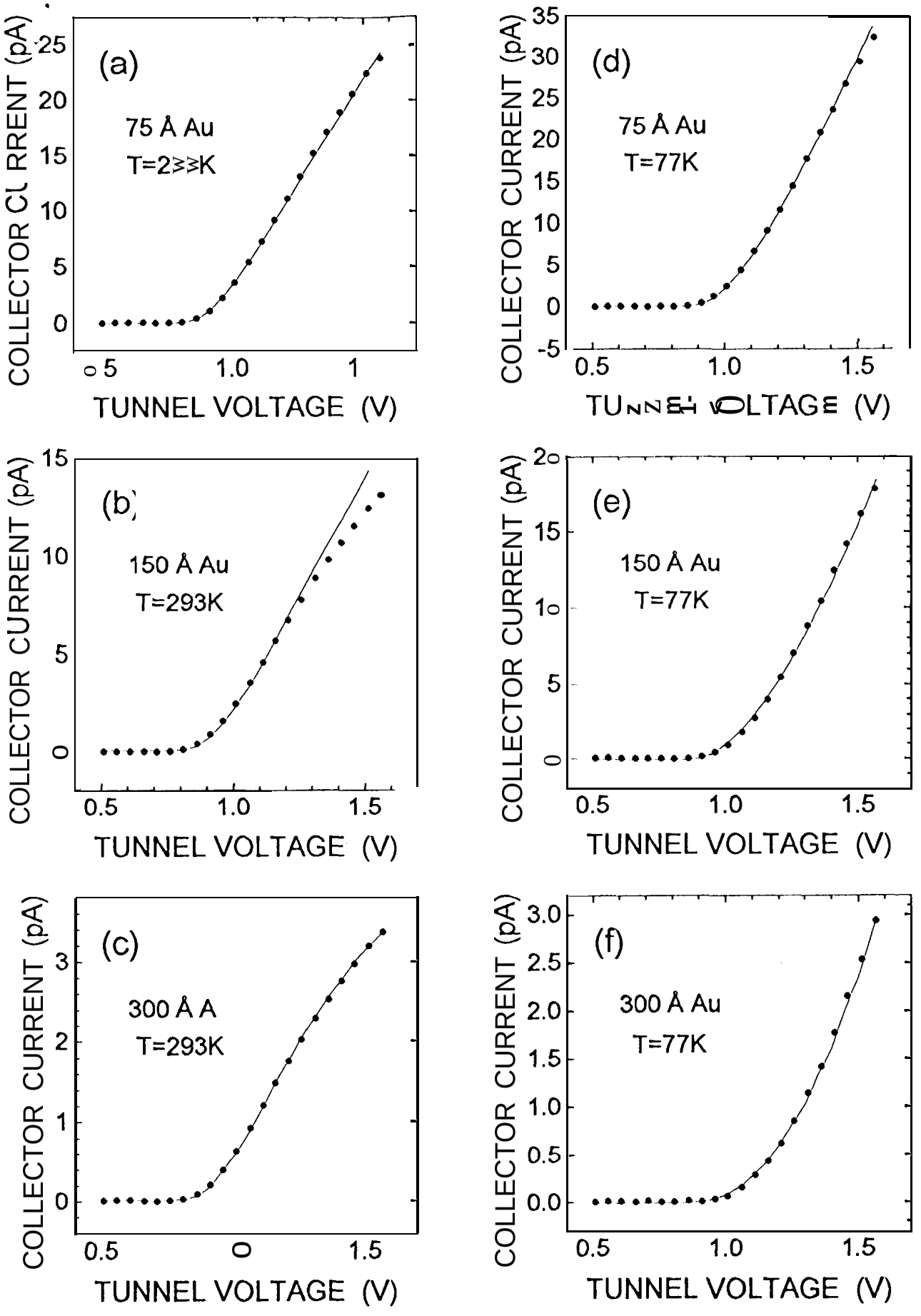
(a)
75 Å Au
T=2≥≥K
COLLECTOR CURRENT (pA)
TUNNEL VOLTAGE (V)
(b)
150 Å Au
T=293K
COLLECTOR CURRENT (pA)
TUNNEL VOLTAGE (V)
(c)
300 Å A
T=293K
COLLECTOR CURRENT (pA)
TUNNEL VOLTAGE (V)
(d)
75 Å Au
T=77K
COLLECTOR CURRENT (pA)
TUNNEL VOLTAGE (V)
(e)
150 Å Au
T=77K
COLLECTOR CURRENT (pA)
TUNNEL VOLTAGE (V)
(f)
300 Å Au
T=77K
COLLECTOR CURRENT (pA)
TUNNEL VOLTAGE (V)

Figure 4

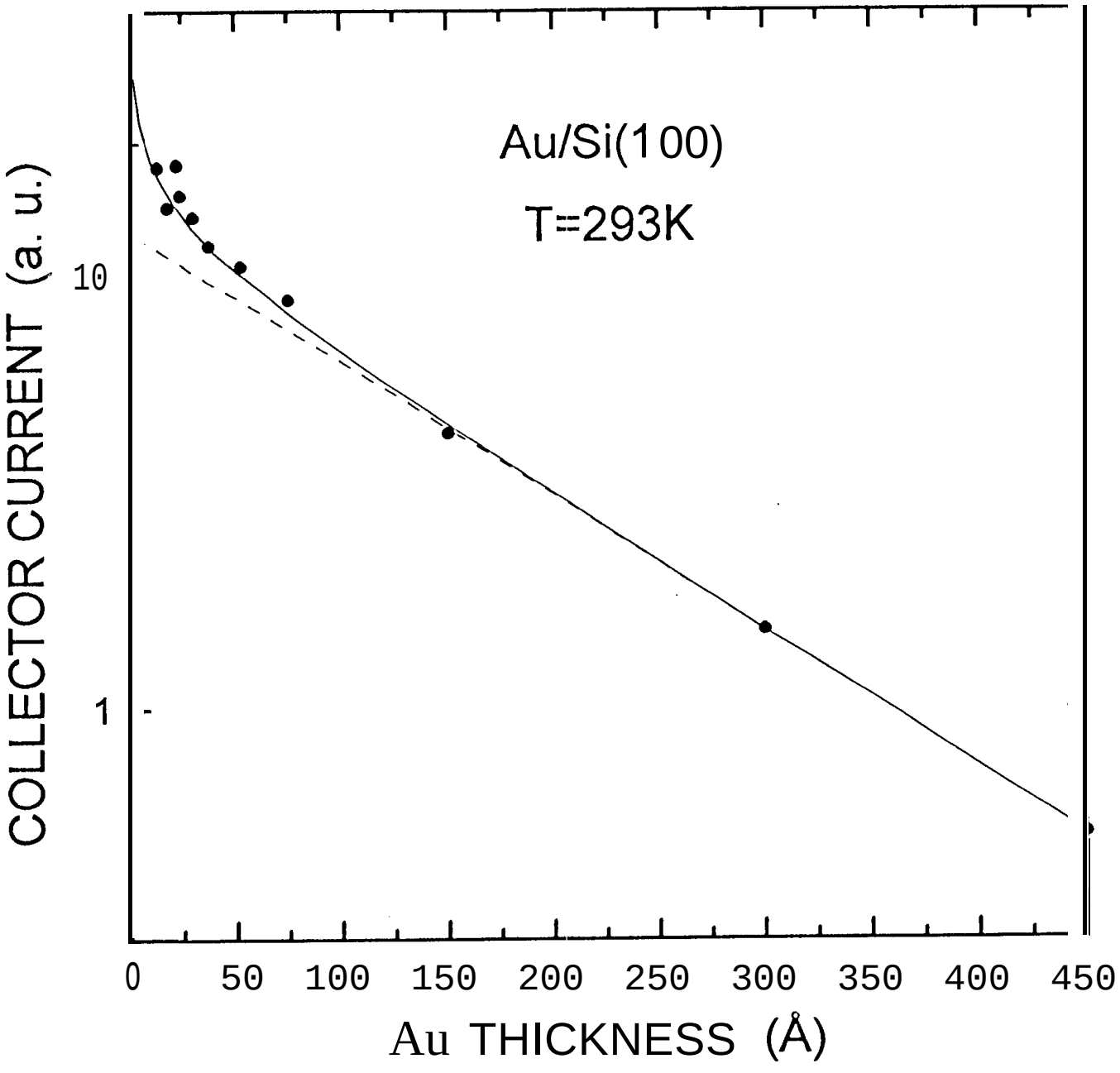
Au/Si(100)
T=293K
COLLECTOR CURRENT (a. u.)
10
1
0
50
100
150
200
250
300
350
400
450
Au THICKNESS (Å)

Figure 5